A coarse-grained polymer model for studying the glass transition

Cite as: J. Chem. Phys. **150**, 091101 (2019); https://doi.org/10.1063/1.5089417
Submitted: 18 January 2019 . Accepted: 10 February 2019 . Published Online: 04 March 2019

Hsiao-Ping Hsu, and Kurt Kremer

The Journal of Chemical Physics | COMMUNICATION | scitation.org/journal/jcp

A coarse-grained polymer model for studying the glass transition

Cite as: J. Chem. Phys. 150, 091101 (2019); doi: 10.1063/1.5089417
Submitted: 18 January 2019 • Accepted: 10 February 2019 •
Published Online: 4 March 2019

Hsiao-Ping Hsu[a] and Kurt Kremer[b]

AFFILIATIONS

Max-Planck-Institut für Polymerforschung, Ackermannweg 10, 55128 Mainz, Germany

[a]hsu@mpip-mainz.mpg.de
[b]kremer@mpip-mainz.mpg.de

ABSTRACT

To study the cooling behavior and the glass transition of polymer melts in bulk and with free surfaces, a coarse-grained weakly semi-flexible polymer model is developed. Based on a standard bead spring model with purely repulsive interactions, an attractive potential between non-bonded monomers is added such that the pressure of polymer melts is tuned to zero. Additionally, the commonly used bond bending potential controlling the chain stiffness is replaced by a new bond bending potential. For this model, we show that the Kuhn length and the internal distances along the chains in the melt only very weakly depend on the temperature, just as for typical experimental systems. The glass transition is observed by the temperature dependency of the melt density and the characteristic non-Arrhenius slowing down of the chain mobility. The new model is set to allow for a fast switch between models, for which a wealth of data already exists.

Polymer materials are omnipresent in our daily life with applications in medicine and technology, as well as "simple" commodities to name a few. Very often these materials are in the glassy state.[1] In the liquid, more rubbery state, the viscosity dramatically increases close to the glass transition temperature T_g in a non-Arrhenius way.[2–5] This slowing down of the chain mobility is of both high scientific and technological interest. Experimentally, T_g of polymers can be determined as such by observing the change in the heat capacity of polymers using differential scanning calorimetry (DSC)[6] or by measuring the thermal expansion coefficient using thermo mechanical analysis (TMA).[7] However, the nature of the glass transition is still not fully understood.[8–13] It is the purpose of this communication to present a most simple, efficient bead spring model (BSM), which allows us to study these effects and which can make contact with the huge body of simulation data available in the literature.

Computer simulations play an important role in investigating the structure and molecular motion (viscosity) of polymeric systems under a variety of different conditions. For studying glassy polymers, both atomistic and coarse-grained models are widely used in the literature.[10,11] The structure and thermal behavior of fluid mixtures can also be analyzed by tuning relative resolution in a recently developed hybrid model combining the fine-grained and coarse-grained models.[14] Our aim is to eventually study generic properties of large and highly entangled polymer melts in bulk, in confinement, and with free surfaces as a function of temperature within accessible computing times. For this, we adopt a highly efficient coarse-grained model.[15] Usually in these models, the excluded volume interaction is taken care of by a purely repulsive Lennard-Jones (LJ) potential, the Weeks-Chandler-Andersen (WCA) potential,[15] which prevents the study of surfaces[16,17] and displays a rather high pressure ($P \approx 5.0\varepsilon/\sigma^3$, $T = 1.0\varepsilon/k_B$, density $\rho = 0.85\sigma^{-3}$ in standard Lennard-Jones (LJ) units of energy and length, and k_B being the Boltzmann factor). To reduce the pressure, the cutoff of the WCA potential for non-bonded pairs of monomers is often doubled from $r_{\text{cut}} = 2^{1/6}\sigma$ to $r_c = 2r_{\text{cut}}$, resulting in $P = 1.0\varepsilon/\sigma^3$.[18–23] The two main shortages of this setting are as follows: (1) There is a small discontinuity in the force at the cutoff making microcanonical runs impossible and (2) the pressure is still not very close to zero. Furthermore, chain stiffness usually is taken into account by a bond bending potential,[24–26] which tends to stretch the chains out with decreasing temperatures.[27] As will be shown below, this leads to rather artificial chain conformations upon cooling, while in experiments, chain conformations only very weakly depend on the temperature.[28,29] Our new coarse-grained model is set to overcome these shortages.

Our starting point is the standard bead spring model (BSM)[15] with a weak bending elasticity[24] (the bending strength $k_\theta = 1.5\varepsilon$)

for which a huge body of data already exists (see, e.g., Refs. 25 and 30–34). While focusing on $k_\theta = 1.5\varepsilon$, our approach easily applies to other bending constants as well. At the standard melt density of $0.85\sigma^{-3}$ (σ being the unit of length), the weak bending elasticity combined with the chain packing result in an entanglement length of only $N_e = 28$ monomers. $N_e = 28$ is small enough to allow for extremely efficient simulations of highly entangled, huge polymeric systems, while at the same time, the subchain of length N_e is already well described by a Gaussian chain. The purpose of this communication is to replace/extend the WCA excluded volume interaction potential to arrive at a pressure of $P = 0.0\varepsilon/\sigma^3$, which allows us to study free surfaces in interaction with gases, liquids, and particles, for example, and to replace the standard bending potential $U_{\mathrm{BEND}}^{(\mathrm{old})}(\theta) = k_\theta(1-\cos\theta)$ by a new modified $U_{\mathrm{BEND}}(\theta)$, which should lead to the typical very weak temperature dependence of chain conformations in melts. The close resemblance to the standard semiflexible bead spring model will allow to switch "on the fly" between the models and to make use of the already broadly available data.

In a first step, we add an attractive well to the WCA excluded volume in order to reduce the pressure in the system from $P = 5.0\varepsilon/\sigma^3$ to $P = 0.0\varepsilon/\sigma^3$. For this, we add $U_{\mathrm{ATT}}(r)$ [see Fig. 1(a)]

$$U_{\mathrm{ATT}}(r) = \begin{cases} \alpha\left[\cos\left(\pi\left(\frac{r}{r_{\mathrm{cut}}}\right)^2\right)\right], & r_{\mathrm{cut}} \le r < r_c^a \\ 0, & \text{otherwise} \end{cases} \quad (1)$$

between all non-bonded monomers. $U_{\mathrm{ATT}}(r)$ is set to not alter the local bead packing. It is chosen to have zero force at the cutoff as well as at the contact point between the two parts of the potential at $r_c = 2^{1/6}\sigma$, which is needed in case microcanonical simulations are performed. As illustrated in Fig. 2(a), adding this term to the standard model equilibrates and reduces the pressure to zero in less than 5τ (τ being the standard LJ unit of time). This time corresponds to a small, local bead displacement of about 1σ, for which the characteristic time is[32] $\tau_0 \approx 2.89\tau$. Furthermore, since the number of particles Z in the interaction range $r_c^a = 1.5874\sigma$ is ≈15 instead of ≈45 at $r_c = 2.25\sigma$ ($P = 1.0\varepsilon/\sigma^3$) or ≈60 at $r = 5.0$ ($P = 0.0\varepsilon/\sigma^3$) using the standard LJ potential, the present model is computationally significantly more efficient. In the next step, we replace the standard bond bending potential $U_{\mathrm{BEND}}^{(\mathrm{old})}(\theta) = k_\theta(1-\cos\theta)$ which would lead to a rod-like chain in the ground state at $T = 0.0\varepsilon/k_B$ by a new bending potential $U_{\mathrm{BEND}}(\theta)$ with the goal to (1) match the chain conformations at $T = 1.0\varepsilon/k_B$ and (2) to approximately preserve them upon cooling. Thus, it should satisfy the condition that the mean square end-to-end distance of chains, $\langle R_e^2\rangle$, does not (preferably) or only very weakly depend on the temperature T. The new bond bending potential $U_{\mathrm{BEND}}(\theta)$ [see Fig. 1(b)] is chosen as

$$U_{\mathrm{bend}}(\theta) = -a_\theta \sin^2(b_\theta\theta), \quad 0 < \theta < \theta_c, \quad (2)$$

with the bond angle θ defined by $\theta = \cos^{-1}\left(\frac{\vec{b}_j\cdot\vec{b}_{j+1}}{|\vec{b}_j||\vec{b}_{j+1}|}\right)$, where $\vec{b}_j = \vec{r}_j - \vec{r}_{j-1}$ is the bond vector between monomers j and $(j-1)$ along the chain. The fitting parameters a_θ and b_θ, and the cutoff $\theta_c = \pi/b_\theta$ where the force $|\vec{F}(\theta = \theta_c)| = 0$ are adjusted such that the estimates of the mean square internal distance $\langle R^2(s)\rangle$ for all chemical distance s between two monomers along the same chain follow the same curve as obtained from the model using $U_{\mathrm{BEND}}(\theta)$ with $k_\theta = 1.5\varepsilon$. Comparing to the reference data for a polymer melt of $n_c = 2000$, $N = 50$ shown in Fig. 2(b), we find that $a_\theta = 4.5\varepsilon$, $b_\theta = 1.5$ lead to an almost perfect match of the two systems. Our data are also in perfect agreement with the theoretical prediction described by a freely rotating chain (FRC) model.[32,35]

Compared to the original model, the profiles of the pair distribution function $g(r)$ of all, inter, and intra pairs of monomers for polymer melts show that the two potentials $U_{\mathrm{BEND}}(\theta)$ and $U_{\mathrm{ATT}}(r)$ only have very small effects on the local packing of monomers [Fig. 2(c)]. The results of the collective structure factor $S(q)$ also show that using the new model, the occurrence of the first peak remains at $q = q^* \approx 6.9\sigma^{-1}$, indicating the same mean distance between monomers in the first neighbor shell of the polymer melt. The peak itself is slightly higher, indicating a slightly more structured local environment, in agreement with the observed weakly enhanced bead friction.

We now turn to the temperature dependency and compare melts of the new model to the standard semiflexible polymer model. For this, we perform molecular dynamics (MD) simulations (Hoover barostat with Langevin thermostat[36,37] implemented in ESPResSo++[38]) at constant temperature T by a stepwise cooling,[20] and constant pressure $P = 0.0\varepsilon/\sigma^3$ ($P = 5.0\varepsilon/\sigma^3$ for the old model), i.e., in the isothermal-isobaric ensemble (NPT), for two polymer melts of $n_c = 2000$, $N = 50$ and $n_c = 1000$, $N = 500$, respectively. The temperature is reduced in steps of $\Delta T = 0.05\varepsilon/k_B$ with a relaxation time between each step of $\Delta t = 60\,000\tau$ resulting in a cooling rate of $\Gamma = \Delta T/\Delta t = 8.3 \times 10^{-6}\varepsilon/(k_B\tau)$. Δt corresponds to $\approx 8.3\tau_{R,N=50} \approx 0.083\tau_{R,N=500}$ ($\tau_{R,N}$ being the Rouse time

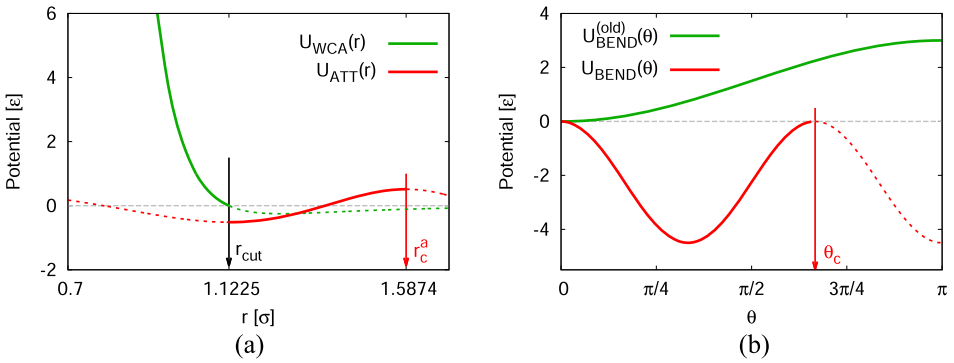

FIG. 1. (a) Non-bonded and short-range repulsive potential $U_{\mathrm{WCA}}(r)$ and attractive potential $U_{\mathrm{ATT}}(r)$ with $\alpha = 0.5145\varepsilon$ [Eq. (1)] plotted as a function of distance r. (b) Standard and new bond bending potentials $U_{\mathrm{BEND}}^{(\mathrm{old})}(\theta)$ with $k_\theta = 1.5\varepsilon$ and $U_{\mathrm{BEND}}(\theta)$ with $a_\theta = 4.5\varepsilon$, $b_\theta = 1.5$ [Eq. (2)], plotted as a function of bond angle θ. In (a) and (b), the cutoff values are pointed by arrows.

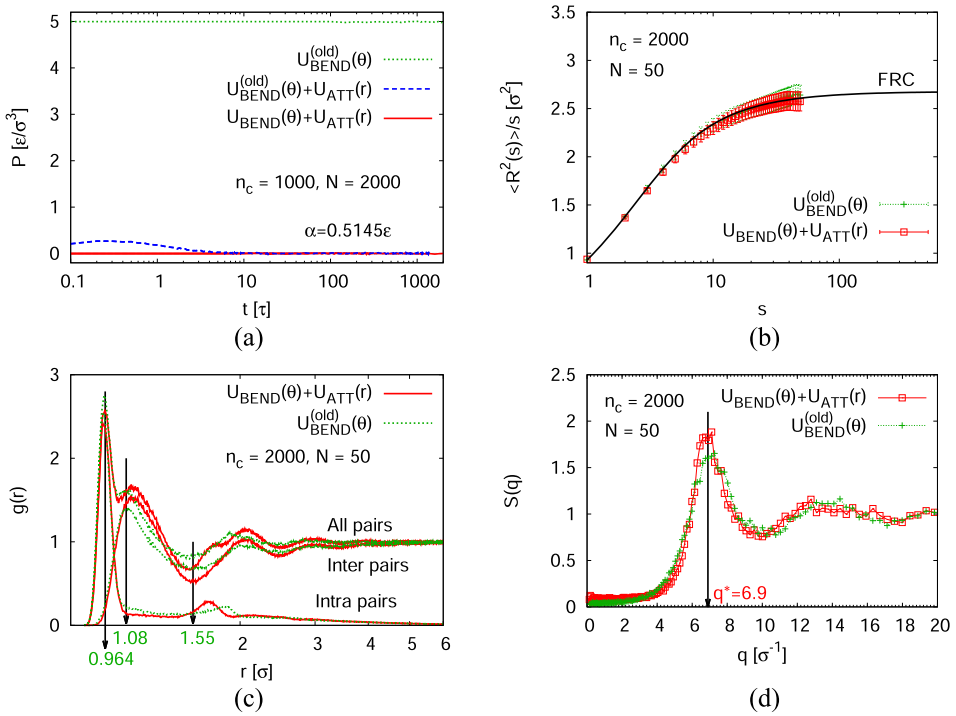

FIG. 2. (a) Pressure P plotted versus the relaxation time t. (b) Rescaled mean square internal distance, $\langle R^2(s)\rangle/s$, plotted versus the chemical distance s between two monomers along the same chain. (c) Radial distribution function $g(r)$ plotted as a function of r for all, inter, and intra pairs of monomers, as indicated. (d) Collective structure factor $S(q)$ plotted versus the wave factor q. Polymer melts at $T = 1.0\varepsilon/k_B$ described by the standard BSM with additional potentials $U^{(old)}_{BEND}(\theta)$, $U_{ATT}(r)$, and $U_{BEND}(\theta)$ are shown, as indicated.

of the chains at $T = 1.0\varepsilon/k_B$ for the old model). The results of the mean square internal distances $\langle R^2(s)\rangle$ and the bond angle probability distribution, $P(\theta)$, are shown in Figs. 3 and 4, respectively.

First, let us focus on the standard weakly semiflexible model. As the temperature decreases, the chains stretch out as displayed in Fig. 3(a) for $N = 50$. While for $N = 50$ the cooling rate is slow enough to allow

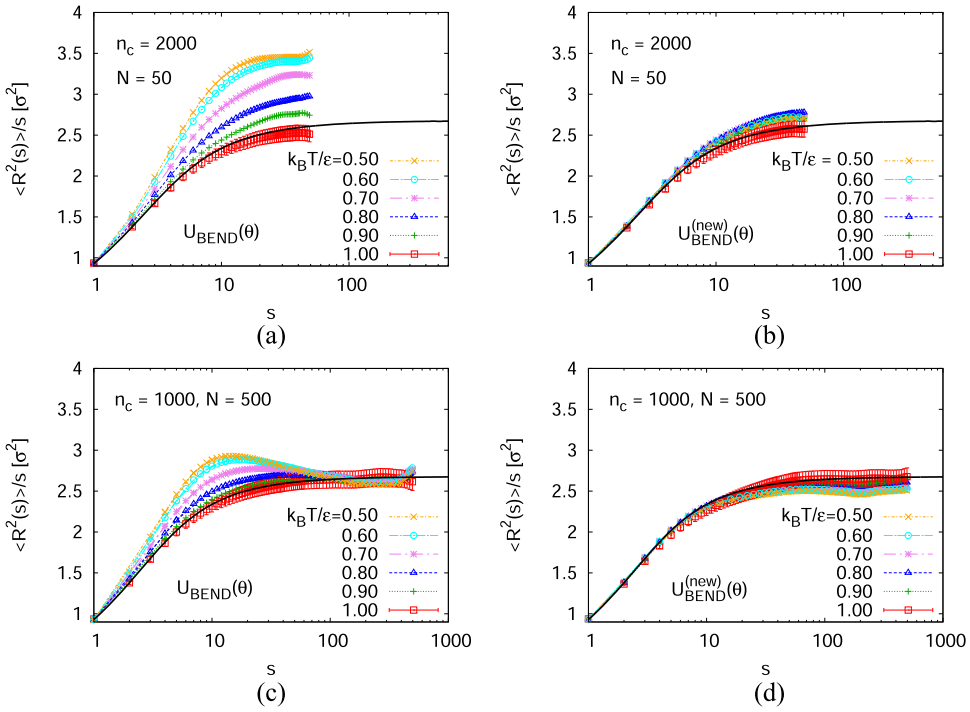

FIG. 3. Rescaled mean square internal distance, $\langle R^2(s)\rangle/s$, plotted as a function of chemical distance s for polymer melts described by the standard BSM with the original and new bond bending potentials $U^{(old)}_{BEND}(\theta)$ [(a) and (c)] and $U_{BEND}(\theta)$ [(b) and (d)], respectively, at $P = 0.0\varepsilon/\sigma^3$. The theoretical prediction for FRC with[32] $\langle\cos\theta\rangle = 0.4846$ estimated for fully equilibrated polymer melts of $n_c = 1000$, $N = 2000$ is also shown for comparison.

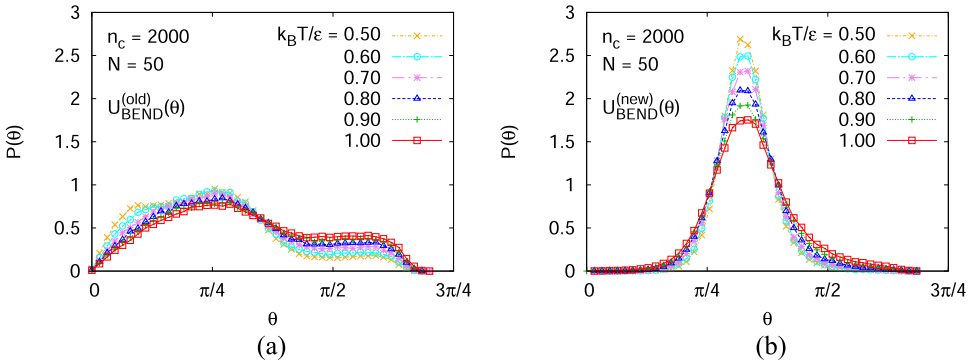

FIG. 4. Probability distribution of bond angle θ for polymer melts described by the standard BSM with the original and new bond bending potentials $U_{\mathrm{BEND}}^{(\mathrm{old})}(\theta)$ (a) and $U_{\mathrm{BEND}}(\theta)$ (b), respectively.

for equilibration over a wide temperature range, for longer chains [$N = 500$, Fig. 3(c)], the system cannot equilibrate anymore even on short length scales ($s \leq 50$), leading to a characteristic maximum in $\langle R^2(s)\rangle/s$. For long chain simulations, it will not be possible to avoid this artefact. Also the strong increase in $\langle R^2(s)\rangle$ of the standard semi-flexible polymer model is an artefact of the model when compared to experiments. This increase in the chain stiffness is related to the shift of the probability distribution $P(\theta)$ towards smaller angles as revealed in Fig. 4(a) and which directly connects to the shape of the standard bending potential.[22] In contrast, the new excluded volume and bending potential not only leads to a conformational very close match with the old one at $T = 1.0\varepsilon/k_B$, but it also avoids a significant temperature shift. Figure 4(b) demonstrates for $N = 50$ that $\langle R^2(s)\rangle/s$ becomes independent of T within the error bars. As a consequence, we also do not observe the maximum in $\langle R^2(s)\rangle/s$ for $N = 500$ as a function of temperature [Fig. 3(d)]. These observations fit to the T dependence of the distribution $P(\theta)$ [Fig. 4(b)], which only becomes somewhat sharper but does not reveal any shift in the maximum.

Finally, we report some preliminary results for our new model in the glass transition region. As we are not interested here in details of the transition itself, we focus on $N = 50$ ($n_c = 2000$) and one cooling rate ($\Gamma = 8.3 \times 10^{-6}\varepsilon/(k_B\tau)$), which, however, allows for a full relaxation of the system up to the region very close to T_g, the observed glass transition temperature. T_g can be determined from the change in density ρ or volume V as a function of temperature.[20] The intersection of linear extrapolation of $\ln V(T)$ between the liquid branch ($\ln V_{\mathrm{liquid}} = a_{\mathrm{liquid}} + \alpha_{\mathrm{liquid}} T$) and the glass branch ($\ln V_{\mathrm{glass}} = a_{\mathrm{glass}} + \alpha_{\mathrm{glass}} T$) gives a good estimate of T_g. Here, α_{liquid} and α_{glass} are thermal expansion coefficients for polymer melts in the liquid state and the glass state, respectively. The results of $\ln V$ plotted versus T are shown in Fig. 5(a). The glass transition occurs

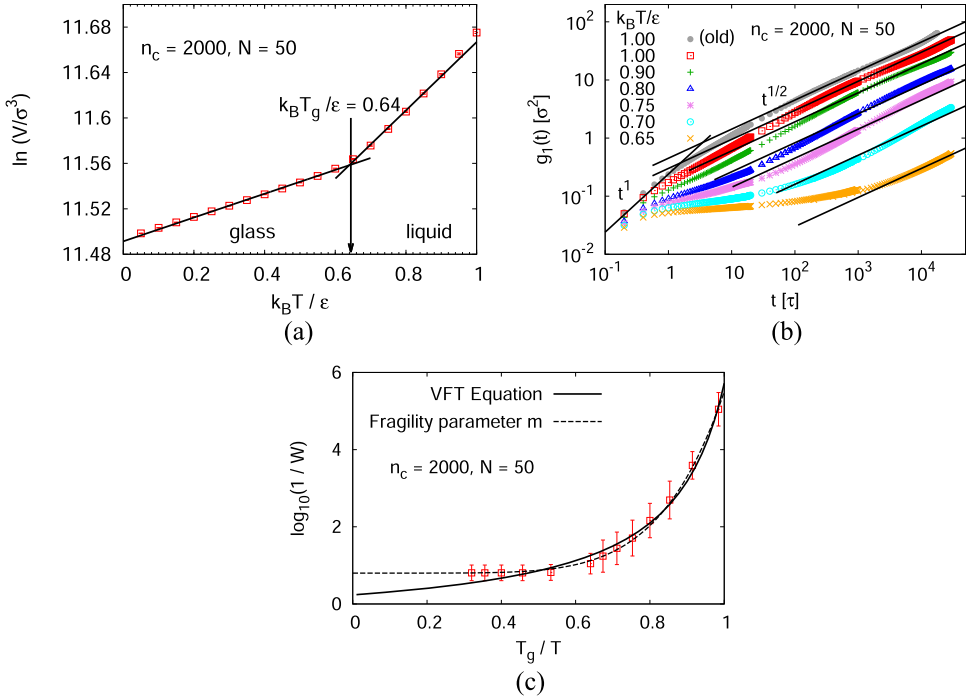

FIG. 5. (a) Logarithm of volume of the system, $\ln V/\sigma^3$, plotted versus temperature k_BT/ε. The two linear lines give the best fit of our data along the liquid branch ($a_{\mathrm{liquid}} = 11.37$, $\alpha_{\mathrm{liquid}} = 0.30k_B/\varepsilon$) and the glass branch ($a_{\mathrm{glass}} = 11.49$, $\alpha_{\mathrm{glass}} = 0.10k_B/\varepsilon$). (b) Time evolution of mean square displacement of inner monomers, $g_1(t)$ at various chosen temperatures T. The predicted scaling laws by the Rouse model are shown by straight lines. (c) Common logarithm of the inverse of the rate constant W estimated from (b), $\log_{10}(1/W)$, plotted versus T_g/T. Data for $k_BT/\varepsilon > 1.0$ are also included here. The temperature dependence of the fragility parameter $m(T) = 4.7(T_g/T)^{6.0} + 0.8$ is shown by a dashed curve, and the VFT equation $\log_{10}(1/W) = A + B/(T - T_0)$ with $A = 0.24$, $B = 0.45\varepsilon/k_B$, and $T_0 = 0.56\varepsilon/k_B$ is shown by a solid curve.

around $T_g = 0.64\varepsilon/k_B$. To investigate the mobility of chains at $T > T_g$, we perform additional NVT MD simulations with a weak coupling Langevin thermostat for polymer melts at k_BT/ε = 1.0, 0.95, 0.90, 0.85, 0.80, 0.75, 0.70, and 0.65. The initial configuration and volume of the polymer melt at each temperature T are taken from the last configuration of the NPT run in the cooling process. According to the Rouse model,[39] the mean square displacement (MSD) of monomers, $g_1(t)$, is expressed in terms of the Rouse rate $W = 12k_BT/(\pi\zeta\sigma^2)$ as $g_1(t) = \sigma^2(Wt)^{1/2}$. Here, $\zeta(\propto D^{-1} \propto \eta)$ being the monomeric friction coefficient is related to the self-diffusion coefficient $D = k_BT/(N\zeta)$ and the viscosity η using the Stokes-Einstein relation. The results of $g_1(t)$ obtained from the average MSD of inner 12 monomers are shown in Fig. 5(b). We also include the data at $T = 1.0\varepsilon/k_B$ for the old model for comparison. The Rouse rate W depending on the temperature is determined by the best fit of a straight line with slope 1/2 going through our data on log-log scales. At $T = 1.0\varepsilon/k_B$, the Rouse rate for the old model ($W = 0.20\tau^{-1}$) is faster than the new model ($W = 0.09\tau^{-1}$). From the well-known Vogel-Fulcher-Tammann (VFT) equation[40–42] $\log_{10}\eta = A + \frac{B}{T-T_0}$, where A, B, and T_0 are constants and T is the absolute temperature, Angell[8,9] has proposed the fragility parameter m, defined by[43] $m = d(\log_{10}\eta)/d(T_g/T)\,|_{T=T_g}$. Thus, plotting $\log_{10}(1/W)$ versus T_g/T in Fig. 5(c), we obtain the characteristic behavior of a polymer approaching the glass transition.

In summary, based on the standard BSM, we have introduced a new non-bonded short range attractive potential $U_{\mathrm{ATT}}(r)$ and bond bending potential $U_{\mathrm{BEND}}(\theta)$ for studying polymer melts subject to cooling. The functional form of these two new interaction potentials also is directly applicable to other standard BSM models with different stiffness[25] just by adjusting the coefficients. By keeping $\alpha = 0.5145\varepsilon$, which results in a density of $0.85\sigma^{-3}$ for all longest ($N = 2000$) systems within the error bars, we get $a_\theta = 4.5\varepsilon$ for $0 \le k_\theta/\varepsilon \le 2.0$, and b_θ = 1.32, 1.40, 1.50, and 1.70 for k_θ/ε = 0.5, 1.0, 1.5, and 2.0, respectively. The new coarse-grained model captures the major features of glass-forming polymers and preserves the Kuhn length as well as internal distances and can also be used to study systems with free surfaces. By construction, it can directly take advantage of the available simulation data of standard BSM models at $T = 1.0\varepsilon/k_B$ and can be applied to the available large deformed polymer melts[33,34] and for understanding the viscoelastic behavior of these polymeric systems.

We are grateful to B. Dünweg for a critical reading of the manuscript. This work was supported by the European Research Council under the European Union's Seventh Framework Programme (FP7/2007-2013)/ERC Grant Agreement No. 340906-MOLPROCOMP. We also gratefully acknowledge the computing time granted by the John von Neumann Institute for Computing (NIC) and provided on the supercomputer JUROPA at the Jülich Supercomputing Centre (JSC), and the Max Planck Computing and Data Facility (MPCDF).

REFERENCES

[1] J. H. Anantrao, J. C. Motichand, and B. S. Narhari, Int. J. Adv. Res. **5**, 671 (2017).
[2] R. H. Boyd, R. H. Gee, J. Han, and Y. Jin, J. Chem. Phys. **101**, 788 (1994).
[3] C. A. Angell, Science **267**, 1924 (1995).
[4] M. Paluch, J. Gapinski, A. Patkowski, and E. W. Fischer, J. Chem. Phys. **114**, 8048 (2001).
[5] L. Berthier and G. Biroli, Rev. Mod. Phys. **83**, 587 (2011).
[6] V. B. F. Mathot, *Calorimetry and Thermal Analysis of Polymers* (Hanser, Munich, 1994).
[7] R. Bird, C. Curtis, and R. Armstrong, *Dynamics of Polymer Fluids*, 2nd ed. (Wiley, New York, 1987).
[8] C. A. Angell, J. Phys. Chem. Solids **49**, 863 (1988).
[9] C. A. Angell, J. Non-Cryst. Solids **131-133**, **Part 1**, 13 (1991).
[10] K. Binder and W. Kob, *Glassy Materials and Disordered Solids* (World Scientific, Singapore, 2005).
[11] J.-L. Barrat, J. Baschnagel, and A. Lyulin, Soft Matter **6**, 3430 (2010).
[12] F. H. Stillinger and P. G. Debenedetti, Annu. Rev. Condens. Matter Phys. **4**, 263 (2013).
[13] M. D. Ediger and J. A. Forrest, Macromolecules **47**, 471 (2014).
[14] A. Chaimovich, C. Peter, and K. Kremer, J. Chem. Phys. **143**, 243107 (2015).
[15] K. Kremer and G. S. Grest, J. Chem. Phys. **92**, 5057 (1990).
[16] B. Dünweg, G. S. Grest, and K. Kremer, in *Conference Proceedings of the IMA Workshop, Minneapolis MN, 1996* (Springer, Berlin, 1997).
[17] A. Kopf, B. Dünweg, and W. Paul, J. Chem. Phys. **107**, 6945 (1997).
[18] C. Bennemann, W. Paul, K. Binder, and B. Dünweg, Phys. Rev. E **57**, 843 (1998).
[19] K. Binder, Comput. Phys. Commun. **121-122**, 168 (1999).
[20] J. Buchholz, W. Paul, F. Varnik, and K. Binder, J. Chem. Phys. **117**, 7364 (2002).
[21] K. Binder, J. Baschnagel, and W. Paul, Prog. Polym. Sci. **28**, 115 (2003).
[22] B. Schnell, H. Meyer, C. Fond, J. P. Wittmer, and J. Baschnagel, Eur. Phys. J. E **34**, 97 (2011).
[23] S. Frey, F. Weysser, H. Meyer, J. Farago, M. Fuchs, and J. Baschnagel, Eur. Phys. J. E **38**, 11 (2015).
[24] R. Everaers, S. K. Sukumaran, G. S. Grest, C. Svaneborg, A. Sivasubramanian, and K. Kremer, Science **303**, 823 (2004).
[25] C. Svaneborg and R. Everaers, e-print arXiv:1808.03503 (2018).
[26] C. Svaneborg, H. A. Karimi-Varzaneh, N. Hojdis, F. Fleck, and R. Everaers, e-print arXiv:1808.03509 (2018).
[27] G. S. Grest, J. Chem. Phys. **145**, 141101 (2016).
[28] M. Wind, R. Graf, A. Heuer, and H. W. Spiess, Phys. Rev. Lett. **91**, 155702 (2003).
[29] L. J. Fetters, D. J. Lohse, and R. H. Colby, in *Physical Properties of Polymers Handbook*, 2nd ed., edited by J. E. Mark (Springer, New York, 2007), Chap. 25, pp. 447–454.
[30] G. Zhang, L. A. Moreira, T. Stuehn, K. C. Daoulas, and K. Kremer, ACS Macro Lett. **3**, 198 (2014).
[31] L. A. Moreira, G. Zhang, F. Müller, T. Stuehn, and K. Kremer, Macromol. Theory Simul. **24**, 419 (2015).
[32] H.-P. Hsu and K. Kremer, J. Chem. Phys. **144**, 154907 (2016).
[33] H.-P. Hsu and K. Kremer, ACS Macro Lett. **7**, 107 (2018).
[34] H.-P. Hsu and K. Kremer, Phys. Rev. Lett. **121**, 167801 (2018).
[35] M. Rubinstein and R. H. Colby, *Polymer Physics* (Oxford University Press, Oxford, 2003).
[36] G. J. Martyna, D. J. Tobias, and M. L. Klein, J. Chem. Phys. **101**, 4177 (1994).
[37] D. Quigley and M. I. J. Probert, J. Chem. Phys. **120**, 11432 (2004).
[38] J. D. Halverson, T. Brandes, O. Lenz, A. Arnold, S. Bevc, V. Starchenko, K. Kremer, T. Stuehn, and D. Reith, Comput. Phys. Commun. **184**, 1129 (2013).
[39] P. R. Rouse, J. Chem. Phys. **21**, 1272 (1953).
[40] H. Vogel, Phys. Z. **22**, 645 (1921).
[41] G. S. Fulcher, J. Am. Ceram. Soc. **8**, 339 (1925).
[42] G. Tammann and W. Hesse, Z. Anorg. Allg. Chem. **156**, 245 (1926).
[43] M. L. F. Nascimento and C. Aparicio, J. Phys. Chem. Solids **68**, 104 (2007).